Lightweight SSD: Real-time Lightweight Single Shot Detector for Mobile Devices

Shi Guo, Yang Liu, Yong Ni and Wei Ni
Jiangsu Automation Research Institute, Lianyungang, China

Keywords: Object Detection, CNN Detectors, Lightweight SSD Object Detector, Circle Feature Pyramid Networks, MBlitenet, Bag of Freebies.

Abstract: Computer vision has a wide range of applications, and the current demand for intelligent embedded terminals is increasing. However, most research on CNN (Convolutional Neural Network) detectors did not consider mobile devices' limited computation and did not specifically design networks for mobile devices. To achieve an efficient object detector for mobile devices, we propose a lightweight detector named *Lightweight SSD*. In the backbone part, we design our *MBlitenet* backbone based on the *Attentive linear inverted residual bottleneck* to enhance the backbone's feature extraction capability while achieving the lightweight requirements. In the detection neck part, we propose an efficient feature fusion network *CFPN*. Two innovative and useful *Bag of freebies* named *BLL loss (Both Localization Loss)* and *GrayMixRGB* are applied to the Lightweight SSD's training procedure. They can further improve detector capabilities and efficiency without increasing the inference computation. As a result, Lightweight SSD achieves *74.4 mAP (mean Average Precision)* with only *4.86M* parameters on PASCAL VOC, being 0.2x smaller yet still more accurate 3.5 mAP than the previous best lightweight detector. To our knowledge, the Lightweight SSD is the state-of-the-art real-time lightweight detector on mobile devices with the edge Application-specific integrated circuit (ASIC). Source Code will be released after paper publication.

1 INTRODUCTION

The CNN-based object detectors are commonly used in practical scenarios, including security monitoring, unmanned driving, searching for free parking spaces via cameras. The detector usually consists of three parts: the backbone, the detection neck part, and the detection part. The backbone part is for feature extraction, the neck part is for feature fusion, and the detection part is for object detection or instance segmentation.

Many networks can be used as a backbone, containing both large networks like Resnet-101 (He et al., 2015) and lightweight networks like Mobilenet (Howard et al., 2017). The lightweight networks mean smaller receptive field, faster running time, and smaller parameters than the large networks. The detection neck part is used to fuse the semantic information and feature information between multiple feature maps, including FPN (Lin et al., 2017), PAN (Liu et al., 2018). It is necessary to use the detection neck part to improve the detector's accuracy rate. For the detection part, the typical examples are one-stage detectors and two-stage detector. One-stage detector directly predicts the classification and localization of the inputs. It is real-time and fast in device with GPU. Famous one-stage detectors are SSD (Liu et al., 2016), YOLO (Redmon et al., 2016, 2017, 2018). Two-stage detector is different from the one-stage detector. In the first step, the two-stage detector predicts if the object in the detection boxes and localization regression, and the second step completes classification and localization.

A two-stage detector with a heavy detection part leads to more accuracy, but it is too much computing overhead to use the two-stage detector in a mobile device.

To balance the mobile device's computing-ability and detector's accuracy, we have to design a detector that operates in real-time on a mobile device. To our knowledge, the best detector for a mobile device should have a lightweight backbone with persuasive receptive field ability, a fused detection neck part, and a one-stage detection part.

Guo, S., Liu, Y., Ni, Y. and Ni, W.
Lightweight SSD: Real-time Lightweight Single Shot Detector for Mobile Devices.
DOI: 10.5220/0010188000250035
In *Proceedings of the 16th International Joint Conference on Computer Vision, Imaging and Computer Graphics Theory and Applications (VISIGRAPP 2021) - Volume 5: VISAPP*, pages 25-35
ISBN: 978-989-758-488-6

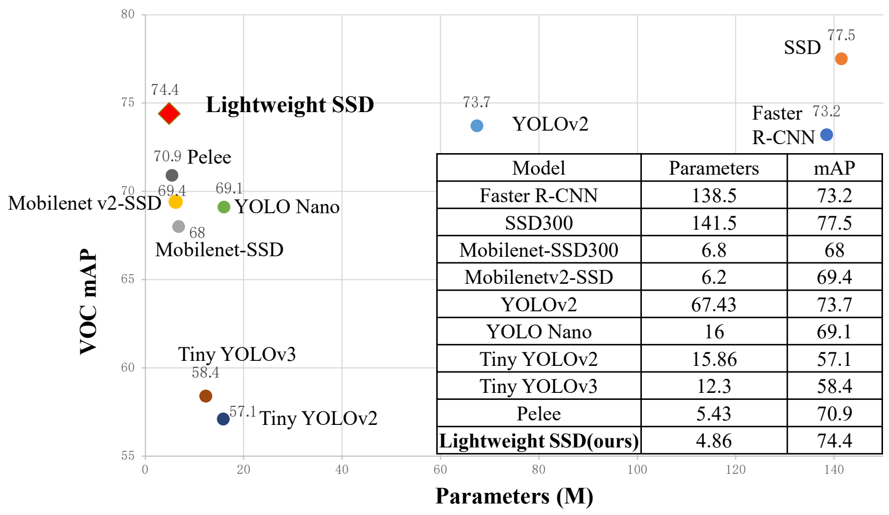

Model	Parameters	mAP
Faster R-CNN	138.5	73.2
SSD300	141.5	77.5
Mobilenet-SSD300	6.8	68
Mobilenetv2-SSD	6.2	69.4
YOLOv2	67.43	73.7
YOLO Nano	16	69.1
Tiny YOLOv2	15.86	57.1
Tiny YOLOv3	12.3	58.4
Pelee	5.43	70.9
Lightweight SSD(ours)	4.86	74.4

Figure 1: Model Parameters vs VOC accuracy - Lightweight SSD achieves 74.4 mAP with only 4.86M parameters on PASCAL VOC, being 0.2x smaller yet still more accurate 3.5 mAP than the previous best lightweight detector Pelee.

This inspires us to design a new lightweight detector named Lightweight SSD. Besides, good detectors in mobile devices should be easy to train in less GPU. This means Bag of freebies methods of object detection during the detector training is indispensable.

This paper aims to design a real-time and lightweight detector for mobile devices. Furthermore, this detector is easy to train in only a few GPUs and easily used. To some extent, anyone who uses one GPU to train and uses the mobile device to test can achieve real-time, high quality results, as the Lightweight SSD results are shown in Fig.1. In summary, our contributions are two-fold:

1. We propose the innovated and efficient object detectors Lightweight SSD. It contains a new lightweight backbone and a new detection neck part whose names are MBlitenet and CFPN (Circle Feature Pyramid Networks), respectively. It makes the detector more accurate in mobile devices and can be trained fast in limited computation, i.e. only one or two 2080Ti GPUs.
2. We verify the influence of “Bag of freebies” methods of object detection during the detector training, like Mosiac (Bochkovskiy et al., 2020), focal loss (Lin et al., 2017). Furthermore, we propose two new Bag of freebies methods, including BLL (Both Localization Loss) and GrayMixRGB. They are useful for the detector's accuracy and not increase the operation parameters.

2 RELATED WORK

Object Detection Models: Object detection refers to identifying whether there is an object of interest from a new image and determining its location and classification. Object detection models are used for object detection, which usually includes one-stage detectors and two-stage detectors. Standard one-stage detectors are SSD (Liu et al., 2016), YOLO (Redmon et al., 2016, 2017, 2018). One-stage detector directly predicts the localization and classification of objects from the bounding boxes in the feature map. On the contrary, a two-stage detector first generates a series of sparse candidate frames on the input image through a heuristic method or a Convolutional Neural Network. It then extracts the feature values of these candidate frame regions. Finally, it predicts localization and classification of objects, such as R-FCN (Region-based Fully Convolutional Network) (Dai et al., 2016), Fast RCNN (Region Convolutional Neural Network) (Girshick, 2015), Faster RCNN (Ren et al., 2015). Intuitively, a one-stage director is an end-to-end object detector and can realize real-time object detection. The two-stage director's processes are complex but have competitive accuracy. In this work, we utilize a one-stage detector that focuses on efficiency because of limited computing ability in a mobile device.

Backbone Networks for Object Detection: To design a lightweight detector, the small backbone networks are necessary. Some famous small networks often are used as the backbone in light detectors, such as Mobilenetv1/v2/v3 (Howard et al., 2017, 2018, 2019), ShuffleNet (Zhang et al., 2018). The Mobilenet series proposed depth separable convolution, which decreases the computing parameters, and the ShuffleNet proposed channel shuffle and grouped convolution also focus on reducing computing. Small networks for classification or object detection's backbone part need different attributes of networks. Therefore, it is not appropriate to directly use a small network for classification as the backbone of object detection. In this work, we consider the drawbacks of previous different lightweight backbone networks and propose a new lightweight backbone named MBlitenet for the lightweight detector.

Detection Neck Part for Detection Models: Detection neck parts mainly represent feature fusion networks, which improve detection accuracy by fusing the feature information from multiple different scale feature maps. Feature fusion networks in object detection attract much research efforts, and there are some feature fusion networks such as FPN (Lin et al.,2017), PAN (Liu et al.,2018), and BiFPN (Tan ET AL.,2020). FPN merges feature information of different scales to form a feature pyramid. PAN and BiFPN combine feature information from a couple of feature pyramids in order. In our work, we propose a circle feature pyramid network (CFPN) to recycle different feature pyramid information for fruitful feature fusion and better object detection accuracy.

Bag of Freebies: A CNN-based object detector contains two procedures: training and inference. Once we have completed the training and obtained a better model, we will use it as the inference model. We can optimize the model to get more accuracy and more accessible training procedure from two aspects: training tricks and some methods only increase training time without increasing inference cost. The above two parts are usually called "Bag of freebies".

The data augmentation uses some methods to make the training dataset bigger. They have more information dimensions for model generalization, such as random erase (Zhong et al., 2017), CutOut (DeVries et al.,2017), and Mosiac (Bochkovskiy et al.,2020). In order to solve the problem of uneven data distribution, another method in Bag of freebies named hard negative example mining (Sung et al., 1998) method is adopted in the training procedure. The last Bag of freebies is designing better loss functions, including Bounding Box regression and classification for improving model accuracy and easy training. Like the focal loss (Lin et al., 2017) method, the classification loss function can balance the negative and positive samples and consider the classification difficulty differences. The traditional Bounding Box regression loss function is L1 loss function, which does not consider the intersection-over-union (IOU) between bounding boxes and ground truth boxes. Therefore, some new Bounding Box regression loss functions that care about the intersection-over-union (IOU) were proposed, such as IOU loss (Yu et al., 2016), GIOU loss (Rezatofighi et al., 2019). In this work, we propose two new Bag of freebies methods, including BLL loss and GrayMixRGB to improve detectors' accuracy.

3 LIGHTWEIGHT SSD

Based on traditional SSD (Single Shot MultiBox Detector), we have developed a new object detector named Lightweight SSD. In this section, we will discuss the detector architecture and some new parts in this detector.

3.1 Lightweight SSD Architecture

The Lightweight SSD architecture is shown in Fig.2, which contains three parts: the backbone, the detection neck part, and the detection part. Fig.2 includes the Bag of freebies in the Lightweight SSD's training process. We proposed a new lightweight backbone named MBlitenet for feature extraction, and a new detection neck part named CFPN (Circle Feature Pyramid Networks) for feature fusion. The detection neck part takes the level 3-7 feature maps from the backbone network and applies the feature fusion. After that, these fused feature maps are fed to the detection part to get the object class and bounding box regression respectively.

3.2 Backbone Network: MBlitenet

In this subsection, we introduce a new lightweight backbone network named MBlitenet. The architecture of MBlitenet is composed of both traditional linear inverted residual bottleneck

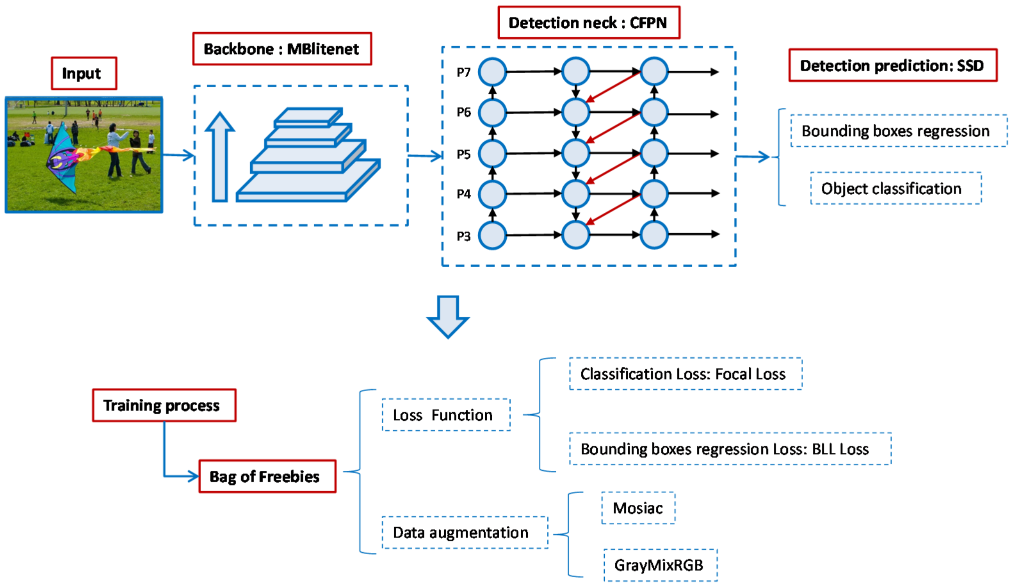

Figure 2: Lightweight SSD Architecture (above) and the Bag of freebies in Lightweight SSD's training process (below).

(Sandler et al., 2018) and the attentive linear inverted residual bottleneck. The detailed convolutional operations inside these two parts are mixed depthwise convolutions that will be introduced in chapter 3.2.2.

3.2.1 Attentive Linear Inverted Residual Bottleneck

We proposed a novel part named Attentive linear inverted residual bottleneck composed of traditional linear inverted residual bottleneck (Sandler et al.,2018) and spatial attention module (SAM) part (Wang et al., 2019).

The traditional linear inverted residual bottleneck performs feature dimensionality expend first, and then feature dimensionality reduction (Sandler et al., 2018). The feature maps after dimensionality reduction use linear functions. Fig.3 shows a traditional linear inverted residual bottleneck in the right side. The spatial attention module part uses the pooling method to merge the channels of feature maps. After that, get an attention map for enhancing the original feature maps.

After adding the spatial attention module part to the traditional linear inverted residual bottleneck, our attentive linear inverted residual bottleneck will focus more attention on the objected area. This solves the problem that the traditional linear inverted residual bottleneck does not have the spatial attention information. And this helps the bottleneck increase the focus on the prominent part of the

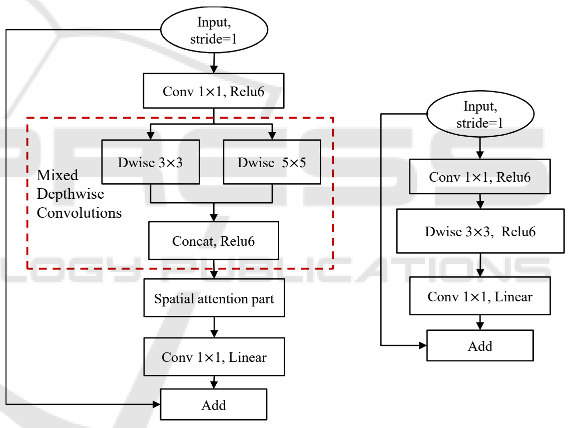

Figure 3: Attentive linear inverted residual bottleneck (left side) and Traditional linear inverted residual bottleneck (right side).

image, thereby improving the detector's object detection accuracy.

Fig.3 shows an attentive linear inverted residual bottleneck in the left. The spatial attention module part is used in the middle of the bottleneck. After the mixed depthwise convolution, the spatial attention module performs average pooling and maximum pooling on the feature maps to obtain two 2-dimensional images. It then merges these two images and uses a standard convolution operation to get the final 2-dimensional spatial attention image. The 2-dimensional spatial attention image obtained by the SAM module is subjected to matrix multiplication with the original feature image. And then the new feature image obtained is used as the input of the next pointwise convolution layer of the network. Table 1 is the operations process of the attentive linear inverted residual bottleneck.

Table 1: Attentive linear inverted residual bottleneck – The dwise represent the depthwise convolution. The *t* represents the expansion factor. The *k* and *k'* represent the output channels and *s* represents stride.

Input	Operation	Output
$h \times w \times k$	1x1 conv2d, ReLU	$h \times w \times (tk)$
$h \times w \times (tk)$	3x3,5x5dwise, ReLU	$\frac{h}{s} \times \frac{w}{s} \times (tk)$
$\frac{h}{s} \times \frac{w}{s} \times (tk)$	spatial attention module	$\frac{h}{s} \times \frac{w}{s} \times (tk)$
$\frac{h}{s} \times \frac{w}{s} \times (tk)$	Linear 1x1 conv2d	$\frac{h}{s} \times \frac{w}{s} \times k'$

3.2.2 Mixed Depthwise Separable Convolutions

Depthwise Separable Convolutional is an efficient block for many lightweight neural network architectures (Howard et al., 2017). Therefore, we use it as a fundamental convolution part of the present work. Depthwise Separable Convolutional includes depthwise convolution and pointwise convolution two parts. The depthwise convolution part applies a single convolutional filter per input channel to realize lightweight. The pointwise convolution is 1×1 convolution, which is used to fuse the features through different channels after depthwise convolution.

Furthermore, to facilitate our module to get a larger receptive field, we use Mixed Convolution (Tan et al.,2019) to replace the traditional depthwise convolution in Depthwise Separable Convolution, and called this new convolution operation Mixed Depthwise Separable Convolution. The architecture of Mixed Depthwise Separable Convolution is in Fig.4. Mixed Convolution means not only use one size kernel filter but apply kinds of different kernel sizes to get a larger receptive field. In this paper, we apply both 3×3 and 5×5 kernel filters in mixed depthwise convolution. The operation is splitting the input tensor into two parts in channels, and one part uses 3×3 kernel's depthwise convolution. The other part uses 5×5 kernel's depthwise convolution. Finally, we merge these two parts to finish mixed depthwise convolution.

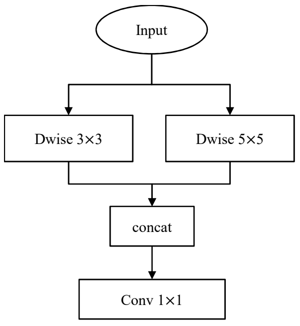

Figure 4: Mixed Depthwise Separable Convolution.

Standard convolution gets an input tensor $D_I \times D_I \times M$, and the output tensor is $D_I \times D_I \times N$. The kernel size is $D_K \times D_K \times M \times N$. The computation cost of standard convolution is $D_I \times D_I \times M \times N \times D_K \times D_K$.

In the same situation, the Mixed Depthwise Separable Convolution has two steps. Firstly, mixed depthwise convolution part's computation cost is equation (1):

$$\begin{aligned}&D_I \times D_I \times M / 2 \times D_{K1} \times D_{K1} + D_I \times D_I \times M / 2 \times D_{K2} \times D_{K2} \\ &= D_I \times D_I \times M / 2 \times (D_{K1} \times D_{K1} + D_{K2} \times D_{K2})\end{aligned} \tag{1}$$

Next, the pointwise convolution part's computation cost is equation (2):

$$D_I \times D_I \times 1 \times 1 \times M \times N \tag{2}$$

The computation cost of Mixed Depthwise Separable Convolution is equation (3):

$$D_I \times D_I \times M / 2 \times (D_{K1} \times D_{K1} + D_{K2} \times D_{K2}) + D_I \times D_I \times M \times N \tag{3}$$

From the equations, it is clear that the Mixed Depthwise Separable Convolution is 7~8 times less computation than the standard convolution.

3.2.3 MBlitenet Architecture

Only one kind of bottleneck cannot fully utilize the feature extraction capabilities of the model. Therefore, the architecture of MBlitenet is in Table 2, which is composed of a traditional linear inverted residual bottleneck, mixed linear inverted residual bottleneck, and attentive linear inverted residual bottleneck. Traditional linear inverted residual bottleneck and attentive linear inverted residual bottleneck have been introduced in chapter 3.2.1. The mixed linear inverted residual bottleneck only replaces the Depthwise Separable Convolutional in traditional linear inverted residual bottleneck to the Mixed Depthwise Separable Convolution.

Table 2: MBlitenet architecture - Each line represents a bottleneck or a regular convolution, repeated *n* times. The *c* represents the output channels of each layer. The first layer of each bottleneck has a stride *s* and all others use stride 1. The *t* represents the expansion factor of each bottleneck.

Input	Operation	t	c	n	s
$300^2\times 3$	conv2d	-	64	1	1
$300^2\times 64$	conv2d	-	32	1	2
$150^2\times 32$	bottleneck	1	16	1	1
$150^2\times 16$	bottleneck	6	24	2	2
$75^2\times 24$	attentive-bottleneck	6	32	3	2
$38^2\times 32$	mix-bottleneck	6	64	4	2
$19^2\times 64$	attentive-bottleneck	6	96	3	1
$10^2\times 96$	mix-bottleneck	6	160	3	2
$5^2\times 160$	attentive-bottleneck	6	320	1	1
$5^2\times 320$	conv2d 1x1	-	1280	1	1
$5^2\times 1280$	Avgpool 5x5	-	-	1	-
$1^2\times 1280$	Conv2d 1x1	-	k	-	

3.3 Detection Neck Part: CFPN

Based on the traditional FPN (Feature Pyramid Networks) (Lin et al., 2017), and think about the actual biological neuron connection process, a specific neuron between different neurons may be the input or output node other neurons. We proposed a new CFPN (Circle Feature Pyramid Networks) that circularly fuses the feature information so that different scales' feature information is better integrated.

The circle feature fusion network of CFPN and traditional FPN are shown in Fig.5(b) and Fig.5(a), respectively. The purpose of CFPN is to fuse feature information of different feature maps scales.

As shown in Fig.5 (b), $P^{in}=(P_3^{in},P_4^{in},...,P_7^{in})$ represents the level of 3-7 feature maps from backbone network, and intermediate fusion layer is $P^{mid}=(P_3^{mid},P_4^{mid},...,P_7^{mid})$. Finally, the output feature maps from CFPN is $P^{out}=(P_3^{out},P_4^{out},...,P_7^{out})$.

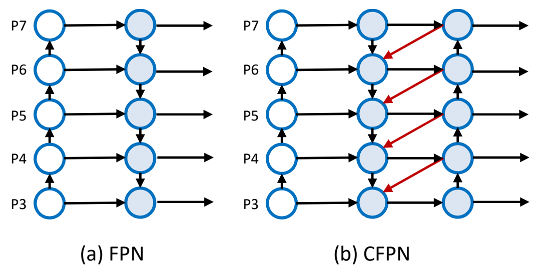

Figure 5: FPN and CFPN feature fusion networks.

The procedure of CFPN (Circle Feature Pyramid Networks) is as follows equation (4):

$$\begin{aligned}
&P_7^{mid}=P_7^{in}\\
&P_6^{mid}=P_6^{in}+\text{Resize}(P_7^{mid})+\text{Resize}(P_7^{out})\\
&...\\
&P_3^{mid}=P_3^{in}+\text{Resize}(P_4^{mid})+\text{Resize}(P_4^{out})
\end{aligned}\tag{4}$$

After obtaining the intermediate layer result, the final output feature fusion result is obtained from the intermediate layer result:

$$\begin{aligned}
&P_7^{out}=Conv(P_7^{mid}+\text{Resize}(P_6^{out}))\\
&P_6^{out}=Conv(P_6^{mid}+\text{Resize}(P_5^{mid}))\\
&...\\
&P_3^{out}=Conv(P_3^{mid})
\end{aligned}\tag{5}$$

where *Resize* is usually upsampling or downsampling for resolution matching, and *Conv* is usually convolution for feature processing.

3.4 Bag of Freebies: BLL Loss and GrayMixRGB

3.4.1 BLL (Both Localization Loss) Loss

The traditional SSD object detection algorithm's loss function contains two parts: classification loss and position regression loss.

The classification loss function has been optimized for Focal loss. For the position regression loss function, the traditional object detection algorithms usually use the Smooth L1 loss function. However, in the evaluation of the detection boxes, the IOU (Intersection over Union) is used to evaluate the prediction box's quality compared with the ground truth box. The Smooth L1 loss and the value of IOU are not equivalent. To solve this problem, Jiahui Yu et al. (Yu et al., 2016) proposed IoU Loss in 2016. However, IoU Loss keeps zero when the prediction box and the ground truth box do not intersect. It cannot reflect the distance between the prediction box and the ground truth box, and it cannot be derived at this time.

To solve the above-mentioned problems of IoU Loss, Zhaohui Zheng et al. proposed DIoU Loss and CIoU Loss (Zheng et al.,2020) in 2020. The formula of DIoU Loss is defined as follows equation (6):

$$DIoU\ loss = 1 - IoU + \frac{\rho^2(a,b)}{c^2} \tag{6}$$

Where, ρ represents the Euclidean distance, a,b represents the center point of the prediction box and ground truth box respectively, c represents the diagonal distance of the smallest bounding rectangle of the prediction box A and the ground truth box B.

The formula of CIoU Loss is defined as follows equation (7):

$$\begin{aligned} CIoU\ loss &= 1 - IoU + \frac{\rho^2(a,b)}{c^2} + \alpha v \\ \alpha &= \frac{v}{(1-IoU)+v} \\ v &= \frac{4}{\pi^2}(\arctan\frac{w^{gt}}{h^{gt}} - \arctan\frac{w}{h})^2 \end{aligned} \tag{7}$$

Where, w^{gt} and h^{gt} represent the width and height of the ground truth box respectively, w and h represent the width and height of the predicted box.

Regarding the IoU Loss, DIoU Loss, and CIoU Loss mentioned above, observing their formulas, we can see that their formulas have common points. They all contain $1-IoU$ part, mainly for the overlap area of the ground truth box and the predicted box. The formula's last part focuses on the center point distance or aspect ratio between the ground truth box and the predicted box. In the position regression loss function, the center point distance and aspect ratio between the ground truth box and the predicted box is the part that the traditional Smooth L1 loss function or L2 loss function are concerned about.

Therefore, we innovatively propose the BothLocalizationLoss (BLL) position regression loss function. Considering the overlap area, center point distance, and aspect ratio of the ground truth box and the predicted box, the formula is simplified as much as possible to facilitate practical application and implementation. The formula is defined as follows equation (8):

$$BothLocalizationLoss = 1 - IoU + \frac{L_2\ loss}{c^2} \tag{8}$$

Where, c represents the diagonal distance of the smallest bounding rectangle of the prediction box and the ground truth box. c^2 helps unify the $L_2\ loss$ and $1-IoU$ to the similar values.

The formula contains both the $1-IoU$ part to focus on the overlapping area of the prediction box and the ground truth box, and the Smooth L1 loss function or the L2 loss function, which is used to focus on the center point distance and aspect ratio between the ground truth box and the predicted box.

The most crucial point is that compared with CIoU Loss, it dramatically reduces the complexity of the formula and the complexity of the implementation code, making it more suitable for multiple applications in the actual field.

3.4.2 Data Augmentation: GrayMixRGB

In this section, we will perform a new data augmentation method named GrayMixRGB. As we all know, the color image and grayscale image of the same picture contain the same objects. This is very easy to recognize for humans. However, it is difficult for the CNN-detector model to maintain the model's robustness, enabling the model to recognize the same target under both grayscale and color images. In order to solve this problem, we propose this new data augmentation method GrayMixRGB. It can make the training set images contain the color information and gray information at the same time.

The process of GrayMixRGB dealing with the training set images is three steps: Firstly, getting an image from the training set. Secondly, replacing the minimum value from the image' RGB values to the gray value. Finally, save the new image. The program code of this process is as follows:

```
begin
  img = RGBimage
  imggray = grayimage
  height = img's height
  width = img's width
  for i,j in range height,width:
    for k in range(3):
   # find the minimum value of RGB
      if img[i,j,k] < min:
        min=minimum of RGB
        index=index of minimum
  if imggray[i,j] > min:
   # change minimum to gray value
     img[i,j,index]=imggray[i,j]
End.
```

3.4.3 Additional Bag of Freebies: Mosaic

We innovatively combine the Mosaic data augmentation method used in YOLOv4 (Bochkovskiy et al., 2020). Mosaic is a data augmentation method by mixing 4 training images. The example is shown in Fig.6. It also mixes the semantics of the four images simultaneously. The purpose is to make the detected targets exceed their general semantics and make the model have better robustness. Simultaneously, doing Mosiac enables the batch normalization (BN) operation during training to count 4 images at a time, which can sufficiently reduce the size of the largest mini-batch during training.

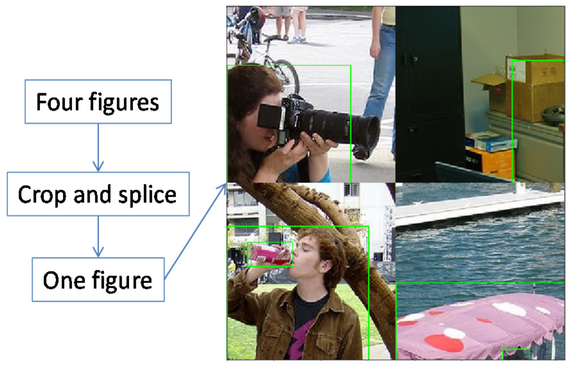

Figure 6: Mosaic data augmentation method.

4 EXPERIMENTS

In this section, we first evaluate the effects of our proposed backbone MBlitenet and the CFPN part with SSD detectors on both MS COCO (test-dev 2017) dataset (Lin et al., 2014) and PASCAL VOC (07+12trainval and 07 test) dataset (Everingham et al.,2010). We then show the performance of the other parts of Lightweight SSD on VOC (07+12trainval and 07test) dataset. Finally, we compare our Lightweight SSD detector to other lightweight detectors on VOC (07+12trainval and 07test) dataset. The deep learning platform uses Tensorflow.

4.1 Evaluation Effect of Backbone and the CFPN

In this paper, we proposed the backbone MBlitenet and the detection neck part CFPN in Lightweight SSD detector. We expect to know how much each of them can contribute to the detector's accuracy and efficiency. Table 3 compares the effect of the backbone MBlitenet and the CFPN in both COCO and VOC dataset. All backbone and detection neck part in Table 3 are based on SSD detector. Starting from the backbone part, our proposed MBlitenet's accuracy is 1.1 mAP better than Mobilenet v2 (Sandler et al., 2018) and 2.5 mAP better than Mobilenet (Howard et al., 2017) in VOC dataset with slightly less parameters. This means the MBlitenet is a better backbone with both good accuracy and lightweight for mobile device. At the same time, our proposed detection neck part CFPN's accuracy is 1.1 mAP better than traditional FPN (Lin et al.,2017) method and 3.5 mAP better than no use feature fusion method. These results suggest that the MBlitenet backbone and the CFPN detection neck part are both essential to our final lightweight Lightweight SSD detector in mobile device.

Table 3: Evaluation effect of Backbone and the CFPN in COCO and VOC - The mAP (VOC) represents the mAP results in VOC dataset. The mAP (COCO) represents the mAP results in COCO dataset. The "-" means no relevant data.

	mAP (VOC)	**mAP (COCO)**	**Parameters**
Mobilenet	68	19.3	6.8M
Mobilenet v2	69.4	21.5	6.2M
Mobilenet v2 + FPN	71.9	-	6.6M
MBlitenet	70.5	**22.3**	**4.16M**
MBlitenet + FPN	72.9	-	4.6M
MBlitenet + CFPN	**74**	-	4.86M

4.2 Evaluation Effect of the Bag of Freebies

In this paper, we proposed two Bag of freebies methods and apply Mosiac method to our detector. We need to evaluate how effective these methods are for our Lightweight SSD detector. The Bag of freebies will not affect the parameters of the detectors, but only affect the accuracy. Therefore, in the comparison experiment, we only focus on accuracy of the detectors. Table 4 compares the effect of different Bag of freebies used in the Lightweight SSD detector on VOC dataset. The basic Lightweight SSD detector contains the MBlitenet backbone, the CFPN detection neck part, and the SSD prediction part. Table 4 shows that after applying BLL Loss as the localization regression loss, the accuracy is improved 0.1 mAP in VOC dataset.

After applying GrayMixRGB data augmentation, the accuracy is improved 0.2 mAP than the basic Lightweight SSD in VOC dataset. The BLL Loss helps the prediction bounding boxes position more exact, and the GrayMixRGB data augmentation makes the dataset contain the gray information that is

Table 5: Lightweight SSD performance on PASCAL VOC.

Model	Backbone	Input	Parameters	mAP
Faster R-CNN	VGG-16	300*300	138.5M	73.2
SSD300	VGG-16	300*300	141.5M	**77.5**
SSD300	Mobilenet	300*300	6.8M	68
SSD300	Mobilenet v2	300*300	6.2M	69.4
SSD300	Mobilenet v2 + FPN	300*300	6.6M	71.9
YOLOv2	Darknet-19	544*544	67.43M	73.7
YOLOv3	Darknet-53	608*608	62.3M	84.1
YOLOv3	Mobilenet	300*300	-	66
YOLO Nano	-	300*300	16M	69.1
Tiny YOLOv2	Tiny Darknet	416*416	15.86M	57.1
Tiny YOLOv3	Tiny Darknet	416*416	12.3M	58.4
ThunderNet	SNet49	320*320	-	70.1
Pelee	PeleeNet	304*304	5.43M	70.9
Lightweight SSD(ours)	MBlitenet + CFPN	300*300	**4.86M**	**74.4**

better for the detector's robustness. However, the Mosaic data augmentation does not perform well in our detector. The reason is that some images after the Mosaic data augmentation will only contain some meaningless ground truth boxes but not real semantic objects in the boxes.

Table 4: Evaluation effect of the Bag of freebies in PASCAL VOC - The "✓" represents the Lightweight SSD detector apply this Bag-of-Freebie. The " - " represents the Lightweight SSD detector does not apply this Bag-of-Freebie.

BLL Loss	GrayMixRGB	Mosaic	mAP
-	-	-	74
✓	-	-	74.1
-	✓	-	74.2
-	-	✓	72.7
✓	✓	-	**74.4**

4.3 Lightweight SSD for Object Detection

We evaluate our Lightweight SSD on PASCAL VOC dataset, which contains the 12+07 trainval data as our training set and 07 test data as our test dataset. The results are exhibited in Table 5. The model is trained using Momentum optimizer with momentum 0.9 and with batch size 126 on 3 Nvidia GeForce RTX 2080 Ti GPUs. The learning rate is the cosine decay learning rate with the base learning rate 0.1, warm up learning rate 0.0333, and the total steps are 500k. For the activation function, we use the ReLU activation. We also apply commonly-used focal loss with α=0.25 and γ=2.0 .

Lightweight SSD exceeds the previous state-of-the-art lightweight detectors. Lightweight SSD achieves 74.4 mAP with only 4.86M parameters on PASCAL VOC, being nearly 30% smaller than the Mobilenet-SSD and surpassing Mobilenet-SSD (Wang et al.,2018) by 6.4 mAP. The Lightweight

SSD also performs better than the Tiny YOLO-series by almost 6 mAP and lighter 50% than Tiny YOLO-series (Redmon et at., 2017). Moreover, Lightweight SSD performs better than the two-stage detector ThunderNet (Qin et al., 2019) by 4.3 mAP. As a result, Lightweight SSD is 0.2x smaller yet still more accurate 3.5 mAP than the previous best lightweight detector Pelee (Wang et al., 2018).

Furthermore, the Lightweight SSD achieves a competitive accuracy to the state-of-art large detectors such as YOLOv2 (Redmon et at., 2017), Faster R-CNN (Liu et al., 2016), and SSD300 (Liu et al., 2016), but really decreases the computation cost.

The models' inference speed in Table 6 is obtained in only 1 Nvidia GeForce RTX 2080 Ti GPU, which can represent the mobile devices with the edge ASIC. Because the edge ASIC means the GPU specially designed for the mobile device

Table 6: The speed for different model on RTX 2080 Ti - The speed represents that the detector infers one image's time.

Model	**Backbone**	**Input**	**Speed (ms)**
SSD300	Mobilenet	300*300	**23**
SSD300	Mobilenet v2	300*300	23.5
SSD300	Mobilenet v2 + FPN	300*300	24
YOLOv3	Darknet-53	608*608	46
Lightweight SSD(ours)	MBlitenet + CFPN	300*300	23.7

From the Table 5 and the Table 6, the Lightweight SSD is compared to a lot of previous detectors in accuracy, parameters and speed. It performs a much better balance between accuracy and computation cost. Lightweight SSD is a very efficient detector to apply on practical mobile devices.

5 CONCLUSIONS

This paper proposes a lightweight and efficient object detector named the Lightweight SSD for mobile devices. In the backbone part, we analyse past lightweight backbone networks and design our MBlitenet backbone based on their advantages and circumvent their shortcomings. In the detection neck part, we propose an efficient feature fusion network CFPN. Two innovative and useful Bag of freebies named BLL loss and GrayMixRGB are applied to the Lightweight SSD detector to further improve detector capabilities and efficiency without increasing the inference computation. Lightweight SSD achieves a very competitive accuracy with particularly less computational cost in mobile devices. We hope to consider an efficient object detector for both arm and edge ASIC model devices in the future.

REFERENCES

Kaiming He, Xiangyu Zhang, Shaoqing Ren, Jian Sun. (2015). Deep Residual Learning for Image Recognition. *In Computer Vision and Pattern Recognition, 2015. CVPR 2015*, abs/1512.03385.

Andrew G. Howard, Menglong Zhu, Bo Chen,Dmitry Kalenichenko, Weijun Wang, Tobias Weyand, Marco Andreetto, and Hartwig Adam. (2017). Mobilenets: Efficient convolutional neural networks for mobile vision applications. *In Computer Vision and Pattern Recognition, 2017. CVPR 2017*, abs/1704.04861.

T. Lin, P. Doll´ar, R. B. Girshick, K. He, B. Hariharan, S. J. Belongie. (2017). Feature pyramid networks for object detection. *In Computer Vision and Pattern Recognition, 2017. CVPR 2017*, abs/1807.03284.

Shu Liu, Lu Qi, Haifang Qin, Jianping Shi, and Jiaya Jia. (2018). Path aggregation network for instance segmentation. *In Proceedings of the IEEE Conference on Computer Vision and Pattern Recognition,2018. CVPR 2018*, pages 8759–8768.

Wei Liu, Dragomir Anguelov, Dumitru Erhan, Christian Szegedy, Scott Reed, Cheng-Yang Fu, and Alexander C Berg. (2016). SSD: Single shot multibox detector. *In Proceedings of the European Conference on Computer Vision (ECCV), 2016*, pages 21–37.

Joseph Redmon, Santosh Divvala, Ross Girshick, and Ali Farhadi. (2016). You only look once: Unified, real-time object detection. *In Proceedings of the IEEE Conference on Computer Vision and Pattern Recognition (CVPR),2016*, pages 779–788.

Joseph Redmon, Ali Farhadi. (2017). YOLO9000: better, faster, stronger. *In Proceedings of the IEEE Conference on Computer Vision and Pattern Recognition (CVPR),2017*,pages 7263–7271.

Joseph Redmon and Ali Farhadi. (2018). YOLOv3: An incremental improvement. arXiv, preprint arXiv:1804.02767.

Alexey Bochkovskiy, Chien-Yao Wang, Hong-Yuan Mark Liao. (2020). YOLOv4: Optimal Speed and Accuracy of Object Detection. *In Proceedings of the IEEE Conference on Computer Vision and Pattern Recognition (CVPR),2020,* arXiv:2004.10934.

Tsung-Yi Lin, Priya Goyal, Ross Girshick, Kaiming He, Piotr Doll´ar. (2017). Focal loss for dense object detection. *In Proceedings of the IEEE International*

Conference on Computer Vision (ICCV),2017, pages 2980–2988.

Jifeng Dai, Yi Li, Kaiming He, and Jian Sun. (2016). R-FCN:Object detection via region-based fully convolutional networks. *In Advances in Neural Information Processing Systems (NIPS),2016*, pages 379–387.

Ross Girshick. (2015) Fast R-CNN. *In Proceedings of the IEEE International Conference on Computer Vision (ICCV), 2015*,pages 1440–1448.

Shaoqing Ren, Kaiming He, Ross Girshick, and Jian Sun. (2015).Faster R-CNN: Towards real-time object detection with region proposal networks. *In Advances in Neural Information Processing Systems (NIPS), 2015*,pages 91–99.

Xiangyu Zhang, Xinyu Zhou, Mengxiao Lin, and Jian Sun. (2018). ShuffleNet: An extremely efficient convolutional neural network for mobile devices. *In Proceedings of the IEEE Conference on Computer Vision and Pattern Recognition (CVPR), 2018*, pages 6848–6856.

Mark Sandler, Andrew G. Howard, Menglong Zhu, Andrey Zhmoginov, and Liang-Chieh Chen. (2018). Mobilenetv2: Inverted residuals and linear bottlenecks. mobile networks for classification, detection and segmentation. *In the IEEE Conference on Computer Vision and Pattern Recognition (CVPR), 2018*, pp. 4510-4520.

Andrew Howard, Mark Sandler, Grace Chu, Liang-Chieh Chen, Bo Chen, Mingxing Tan, Weijun Wang, Yukun Zhu, Ruoming Pang, Vijay Vasudevan. (2019). Searching for mobilenetv3. *In Proceedings of the IEEE International Conference on Computer Vision ICCV*, 2019, arXiv:1905.02244.

Mingxing Tan, Ruoming Pang, and Quoc V Le. (2020). EfficientDet: Scalable and efficient object detection. *In Proceedings of the IEEE Conference on Computer Vision and Pattern Recognition (CVPR), 2020.*

Zhun Zhong, Liang Zheng, Guoliang Kang, Shaozi Li, and Yi Yang. (2017). Random erasing data augmentation. ArXiv preprint arXiv:1708.04896, 2017.

Terrance DeVries and Graham W Taylor. (2017). Improved regularizationb of convolutional neural networks with CutOut. arXiv preprint arXiv:1708.04552, 2017.

K-K Sung and Tomaso Poggio. (1998). Example-based learning for view-based human face detection. *IEEE Transactions on Pattern Analysis and Machine Intelligence (TPAMI),1998*, 20(1):39–51.

Jiahui Yu, Yuning Jiang, Zhangyang Wang, Zhimin Cao, and Thomas Huang. (2016). UnitBox: An advanced object detection network. *In Proceedings of the 24th ACM international conference on Multimedia, 2016*, pages 516–520.

Hamid Rezatofighi, Nathan Tsoi, JunYoung Gwak, Amir Sadeghian, Ian Reid, and Silvio Savarese. (2019). Generalized intersection over union: A metric and a loss for bounding box regression. *In Proceedings of the IEEE Conference on Computer Vision and Pattern Recognition (CVPR), 2019*, pages 658–666.

TiancaiWang, Rao Muhammad Anwer, Hisham Cholakkal, Fahad Shahbaz Khan, Yanwei Pang, and Ling Shao. (2019). Learning rich features at high-speed for single-shot object detection. *In Proceedings of the IEEE International Conference on Computer Vision (ICCV), 2019*, pages 1971–1980.

Mingxing Tan, Quoc V. Le. (2019). MixConv: Mixed Depthwise Convolutional Kernels. *In the British Machine Vision Conference (BMVC), 2019*, arXiv:1907.09595.

Zhaohui Zheng, Ping Wang, Wei Liu, Jinze Li, Rongguang Ye, and Dongwei Ren. (2020). Distance-IoU Loss: Faster and better learning for bounding box regression. *In Proceedings of the AAAI Conference on Artificial Intelligence (AAAI)*, 2020.

Tsung-Yi Lin, Michael Maire, Serge Belongie, James Hays, Pietro Perona, Deva Ramanan, Piotr Doll´ar, and C Lawrence Zitnick. (2014). Microsoft COCO: Common objects in context. *In Proceedings of the European Conference on Computer Vision (ECCV)*,2014.

M. Everingham, L. Van Gool, C. K. Williams, J. Winn, and A. Zisserman. (2010). The pascal visual object classes (voc) challenge. *International journal of computer vision, 2010*,88(2):303–338.

Zheng Qin, Zeming Li, Zhaoning Zhang, Yiping Bao, Gang Yu, Yuxing Peng, Jian Sun. (2019). ThunderNet: Towards Real-time Generic Object Detection. *In Proceedings of the IEEE Conference on Computer Vision and Pattern Recognition (CVPR),2019*, arXiv:1903.11752.

R. J. Wang, X. Li, and C. X. Ling. (2018). Pelee: a real-time object detection system on mobile devices. *In Advances in Neural Information Processing Systems, 2018*, pages 1963–1972.